China Petroleum Processing and Petrochemical Technology

Catalyst Research Volume 23, Issue 2, December 2023 Pp. 4747-4762

# EFFECT OF FLUID VISCOSITY AND FILLING CAPACITY ON PERFORMANCE OF SINGLEINPUT AND TWO INPUTS FLUID COUPLING IN POWER TRANSMISSION SYSTEM

**V.Narasimha Reddy**

Department of Mechanical Engineering, Malla Reddy College of Engineering, Hyderabad, Telangana State, India

**V.Madhusudana Reddy**

Department of Electrical and Electronics Engineering, Malla Reddy Engineering College, Maisammaguda, Secunderabad, Telangana State, India.

**T.Sanjeeva Rao**

School of Engineering, Malla Reddy University, Secunderabad, Telangana State, India.

**Thammireddi V Subhashini**

Department of Electrical and Electronics Engineering, ANITS College,Visakapatnam, Andhrapradesh, India.

**Kannan Shanmugam**

School of Computing Science and Engineering, VIT Bhopal University, Bhopal-Indore Highway, Kothrikalan, Sehore, Madhya Pradesh,India.

***Corresponding Author:** V.Narasimha Reddy

*Department of Mechanical Engineering, Malla Reddy College of Engineering, Hyderabad, Telangana State, India.

**Abstract:**

This study examines the performance characteristics of a Hybrid Fluid Coupling and Fluid Coupling in order to evaluate their effectiveness and efficiency in power transmission systems. The investigation focuses on fluids with varying viscosities and varied filling capacities. A dedicated prototype has been created and constructed for the purpose of conducting performance tests. The aim of this study is to design and optimize a fluid coupling system that can effectively transmit mechanical power while minimizing transmission losses. The fluid couplings are capable of transferring power from both single and dual inputs. The inputs may consist of an Induction motor or any alternative power source, which may afterwards be transmitted to the output shaft via the utilization of a Fluid coupling. When it comes to features like efficient shock, load, and torsional vibration damping, fluid couplings outperform mechanical couplings. Since there is no mechanical interface between the Impeller (the source of input) and the Runner (the destination of the power), acceleration is smooth and the transmission of power is wear-free. An investigation and analysis are conducted on the impact of input power sources, fluids with varying viscosities, and fluid filling percentages in the Fluid Coupling on the resulting output power.

**Keywords:** Fluid coupling, Impeller, Runner, fluid viscosity and Fluid filling capacities.

## Introduction:

The fluid coupling primarily comprises an impeller, a runner, and a working fluid contained within a sealed chamber, and functions based on the hydrokinetic theory. The operation of this system is characterized by the absence of any physical touch between the pushing and driven shafts. The driving wheel functions as a pump impeller, transferring the rotational energy to the working fluid. The driven wheel, on the other hand, functions as a turbine runner, capturing the angular momentum that is transferred from the working fluid. Consequently, the transmission of shaft torque between the driving pump rotor and the driven rotor runner is achieved without any physical contact, thanks to the fluid medium involved in the process. Froude [1] conducted the first groundbreaking work on the idea of hydrodynamic transmission, and in 1877, the Institution of Mechanical Engineers read an article of research on hydrodynamic dynamometers. The earliest hydrodynamic power transmission is credited to Fottinger [2], who filed patents in 1905 detailing both the fluid coupling and the hydrodynamic converter. The international rights for the "Vulcan Coupling" to be used in industry and automotive applications were acquired by Harold Sinclair [3] and the Related Machinery Corporation of England in 1929, marking the starting point of the fluid coupling's use in these fields.

According to Bilton (4), the speed variable fluid clutch operates by adjusting the level of fluid in the internal circuit through the use of leak-off valves. Heldt (2015) devised a hydraulic connection that exhibits a straightforward construction, functioning, and explanation, devoid of any complexities. The impeller and runner components are contained within a fluid-filled housing and ultimately achieve a rotational velocity that closely approximates that of the impeller. Patki et al. (6) investigated the impact of the number of vanes on torque transmission. In a study conducted by Uchiyama et al. [7], it was demonstrated that the relationship between torque and speed exhibit a high degree of sensitivity to minor alterations in operational parameters. The findings for various operational circumstances are validated by Middelmann et al. [8]. In their study, Bai et al. (2019) investigated the augmentation of torque output by the utilization of angled vanes. In their study, Tanaji et al. (10) conducted research on the use of fluid coupling in mopeds. Through experimental analysis, they provided empirical evidence to support the claim that the power transmission capacity of fluid coupling is enhanced to 82% under heavier loads, in contrast to the 76% efficiency seen in centrifugal clutches. Moreover, there will be a further increment of 5% in the aforementioned percentage range, namely from 82% to 87%, provided that the design and manufacture of the fluid coupling are executed with optimal efficiency. The present study

showcases the computational fluid dynamics (CFD) solutions conducted by Zixiang et al. [11] in order to analyze heat transfer and unsteady flow phenomena inside model fluid couplings.
The factors under investigation encompass the cooling via flow, the impact of coupling size, the number of vanes, and the angle of vanes. In their study, Jain et al. (2012) conducted research on the behavior of water and viscous fluid in a fluid coupling, specifically focusing on the filling capacity and its relationship with viscosity. The researchers successfully determined the impact of viscous on the overall performance of the fluid coupling. In their study, Patel et al. (2013) designed a fluid couplings using Pro-E model and conducted an analysis of the obtained data using the software "ANSYS". The researchers investigated the impact of different fluids on the power supply and output speed of the fluid coupling, and found that these parameters are influenced by the speed of the input of the fluid coupling, assuming a consistent quantity and type of oil. The experimental experiments and design innovations conducted by Wallace et al. [14] continue to be extensively utilized in contemporary research.
The fluid dynamics inside the couplings exhibit intricate behavior, particularly when operating under conditions of partial filling or cavitation. The authors Ishihara et al. (2015) demonstrated the viewing of flow patterns within fluid couplings that are partially filled. This was achieved by employing a transparent apparatus including rectangular sections of varying sizes. The study conducted by Uchiyama et al. [16] examines the relationship between fluid coupling performance and speed ratio as well as filling capacity in flow visualization. The study conducted by Mohinoddin et al. (2017) investigated hybrid vehicles that utilize both thermal and electrical power sources. The primary emphasis of their research was the design of a hydraulic transmission system, employing Computational Fluid Dynamics as a tool for analysis. The computational fluid dynamics (CFD) research indicates that the effectiveness of torque transfer in the hybrid fluid coupling has a positive correlation with two factors: (a) decreased clearances between the rotating disks, and (b) lower rotational speed of the engine and motor disks.

The fluid coupling model was established by Danish et al. [18] using the solid work program. This was achieved by modifying the spacing among the driver and driven shafts in order to determine the efficiency. The conclusion was reached by means of minimization. In a research conducted by Sakran et al. (2019), a numerical investigation was performed to determine the pressure characteristics of a centrifugal pump under three distinct scenarios. Each condition maintained identical operating parameters, but varied in the number of blades employed, ranging from five to sixteen. The simulation yielded outcomes that were deemed to be rational and logical. The pressure exhibits a discernible increase when a predetermined number of blades is employed, followed by a subsequent reduction. Therefore, it can be observed that centrifugal pumps exhibit optimal performance when operating with specified blade numbers that correspond to their exact characteristics. In their study, Ramkumar et al. (2020) investigated the effects of revising the design of a radial flow impeller on its performance. Specifically, they explored the impact of altering either the blade width or the angle using plastic material. The researchers found that these design alterations resulted in a substantial rise in the output flow.

The two-way axial-flow pump was investigated by Ji Pei et al. (21). The occurrence of vibration in the impeller is facilitated by the presence of an unsteady flow, which poses a hindrance to the secure functioning of the pump. Rao [22] conducted the initial comprehensive quantitative analysis on dynamometers. The presenter conducted a comprehensive study of the flow route in a filled machine, taking into account several factors such as blade angle, torus form and dimensions, fluid characteristics, and loss coefficients. The primary focus of this analysis was to determine the impact of these variables on the torque ability number. The study conducted by Knudsen et al. [23] focused on the hydrodynamic aspects of axial flow hydraulic generators in order to mitigate cavitation. Additionally, the researchers put out a proposal for an experimental research program on dynamometers. In their study, Mitsuhashi et al. (24) documented a noteworthy vibration issue observed in Froude type machines, which was attributed to the interaction between the rotor and stator vanes. By augmenting the quantity of rotor vanes, the vibration was nearly eradicated. Rolewicz [25] constructed a set of hydrostatic dynamometers in order to evaluate different elements of a military vehicle equipped with four-wheel drive.

The system included pumps for the purpose of extracting energy from various components, while a servo valve was utilized to regulate a hydraulic motor responsible for supplying power to components without inherent power sources. In their study, Longstreth et al. (26) constructed a cost-effective high-bandwidth the dynamometer with the capability to generate a diverse range of torques. For teaching reasons, Holland et al. [27] constructed a cheap absorbent hydrostatic dynamometer for testing smaller and medium-sized engines. To simulate the operation of a hybrid powertrain, Wang et al. [28-29] built a hydrostatic engine dynamometer. The hydraulic dynamometer is considered to be a promising choice for next-generation dynamometers because to its advantageous characteristics, including high power density, low motion, and wide bandwidth. The goal of the current study is to examine a number of variables that impact fluid coupling performance for both single and two inputs. The factors being examined in this study include fluid properties with different viscosities, the amount of fluid filled in the fluid coupling, and the speed ratio between the driving and driven parts.

**Description of Test model setup:**

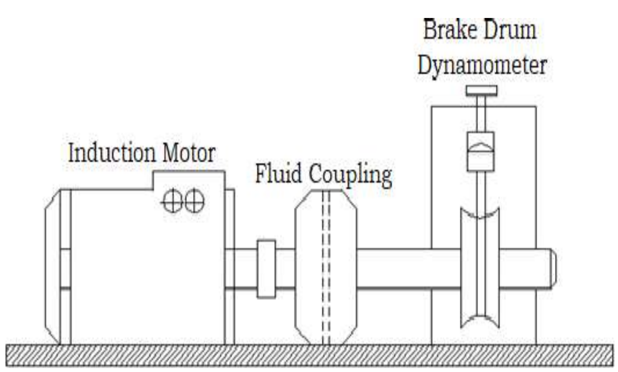


**Fig. 1:** Single Input Fluid Coupling Test setup

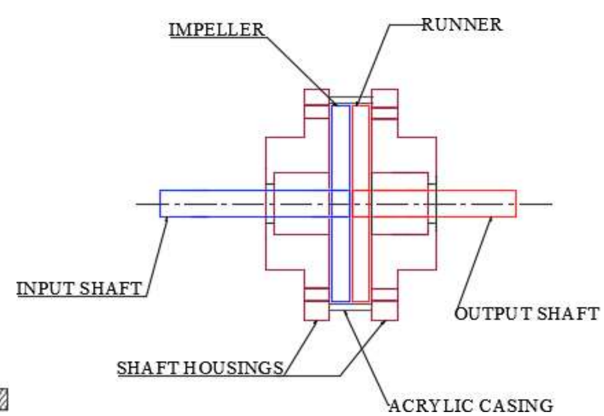


Fig. 2: Schematic diagram of Single nput Fluid Coupling

There is very little space among the trailing and leading edges of the pump's impeller and the turbine runner, and the two are positioned side by side. A commonly employed impeller/runner design in traditional pumps or turbines consists of 24 radial vanes with a face angle of 150 degrees. Figures 1 and 2 depict a standard single input fluid coupling. The impeller is mechanically linked to the input shaft, which is in turn paired with an induction motor. The runner, on the other hand, is connected to the output shaft, which is also linked to a brake dynamometer. The figure 3 and figure 4 illustrate a standard hybrid fluid coupling with two inputs. The first impeller is linked to the exterior input shaft, while the second impeller is attached to the interior input shaft. The runner is mechanically linked to the output shaft, which in turn is hooked to a brake dynamometer.

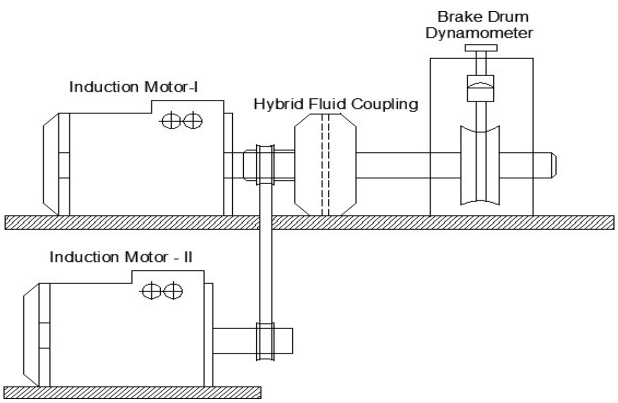


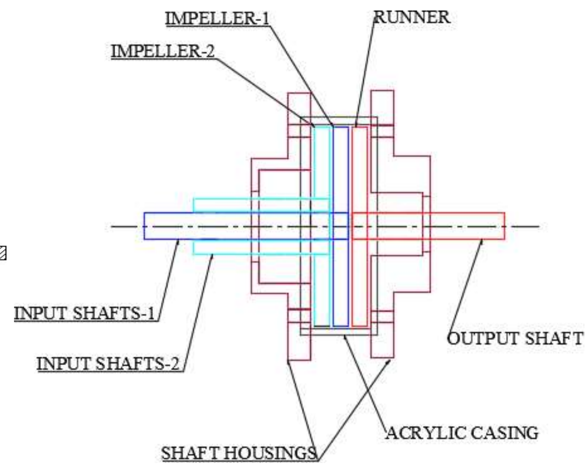


Fig. 3: Two Inputs Fluid Coupling Test setup

Fig. 4: Schematic diagram of Two Inputs Fluid Coupling

The test configuration for the performance test comprises the following components:

**Motor:** The electric motor serves as the primary driving mechanism for the experimental configuration. The technical characteristics of the motor are described below in Table 1.

Catalyst Research Volume 23, Issue 2, December 2023 Pp. 4747-4762

**Table : 1** Technical characteristics of the motor

| | | | |
|---|---|---|---|
| Input Power of the Motor-1<br>Number of poles | 0.5 HP<br>4 | Input Power of the Motor-2<br>Number of poles | 0.25 HP<br>4 |
| Speed | 1500 RPM | Speed | 1500 RPM |
| Power Factor | 0.85 | Power Factor | 0.85 |
| Frequency | 50 Hz | Frequency | 50 Hz |
| No of phase | Single Phase | No of phase | Single Phase |
| Rated voltage | 240 V | Rated voltage | 240 V |
| Rated current | 3.0 A | Rated current | 3.0 A |

**Brake Drum Dynamometer:** Design specifications of the dynamometer are as follows

| | |
|---|---|
| Speed | Up to 1500 RPM |
| Type | Brake Dynamometer-Belt type |
| Cooling | Water cooled |
| Brake Drum Diameter | 120 mm |
| Belt thickness | 6 mm |

**Fluid Coupling:** The elements of the fluid coupling, as well as the standards utilized in this experiment, are outlined below.

Catalyst Research Volume 23, Issue 2, December 2023 Pp. 4747-4762

**Impellers/Runner:**

| | |
|---|---|
| Outer Diameter | 127 mm |
| Dia. of Impeller Eye | 65 mm |
| No. of Vanes | 24 |
| Length of Vane | 31 mm |
| Width of Vane | 10 mm |
| Thickness of Vane | 1.5 mm |
| Face Angle of the Vane | 150 |

**Shaft (Impeller-I and Runner)**

| | |
|---|---|
| Length | 140 mm |
| Diameter | 30 mm |

**3. Casing (Acrylic)**

| | |
|---|---|
| Outer Diameter | 139 mm |
| Inner Diameter | 130 mm |
| Thickness | 5 mm |
| Length | 49 mm |

**4. Shaft (Impeller-II)**

| | |
|---|---|
| Length | 87 mm |
| Outer Diameter | 35 mm |
| Inner Diameter | 30 mm |

**5. Impeller/ Runner H using**

| | |
|---|---|
| Outer Diameter | 170 mm |
| Inner Diameter | 130 mm |
| Groove depth | 5 mm |

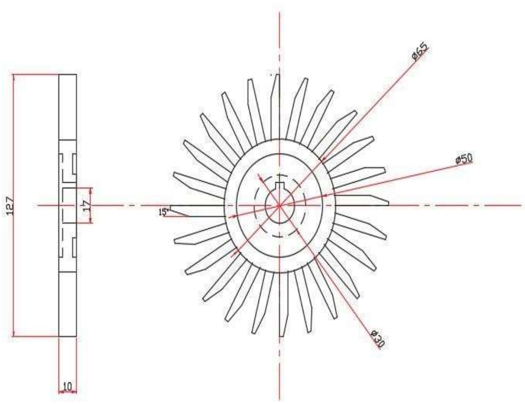


Fig. 5: Impeller/Runner Fig.6: Schematic diagram of Impeller/Runner

**Working Fluid:**

The selection of the working fluid for the fluid couplings is a crucial parameter in the system. The determination of the viscosity of the fluid is conducted by the Society of Automotive Engineers (SAE). Kinematic viscosity is a more common name for viscosity and is generally expressed in stokes (St) or centistokes (1 St = 0.01 cSt). As the numerical value increases, so does the level of viscosity. A substance with high viscosity exhibits a greater degree of resistance to flow, whereas a substance with low viscosity demonstrates a lesser degree of resistance to flow. The relationship between viscosity and temperature is inversely proportional. The viscosity of a substance is also influenced by changes in pressure. An rise in pressure leads to a corresponding increase in viscosity, thereby enhancing the oil's load bearing ability. This study investigates the performance of SAE 10, SAE 20, SAE 40, and SAE 90 oils under varying filling capacities.

**Step by step process of Test:**

The next section provides a comprehensive outline of the step-by-step approach for conducting a performance test.

1. SAE 10 oil should be placed into the SIF coupling. The amount of oil is measured in order to determine a certain percentage of oil.
2. Initiate the activation of the motor and allow for a period of time to elapse until it attains a state of equilibrium. Subsequently, proceed to introduce the load onto the Dynamometer. It is advisable to delay any action until the speed has achieved a level of equilibrium. Take note of the dynamometer load, input and output RPM measurements.
3. Please proceed to alter the load applied to the dynamometer and afterwards document all the recorded measurements once more.
4. Cease the operation of the motor and proceed to augment the volume of oil within the fluid coupling in order to get the desired level of filling capacity. Subsequently, execute the test in accordance with the previously provided instructions.
5. Next, proceed to detach the fluid couplings from the bench that will be tested and proceed with the task of filling it with various fluids such as SAE 20, SAE 40, and SAE 90. Following this, perform the identical testing technique as previously conducted.
6. Please replicate the identical testing methodology for the Two Inputs Fluid Coupling as well.

**Results and Discussions.**

The performance test was conducted using a range of viscous fluids at varying filling capacities, and the outcomes are illustrated in Figures 7 to 10.

**Velocity ratios for different viscous fluids at varying filling capacity for single-input and dual-input fluid couplings:**

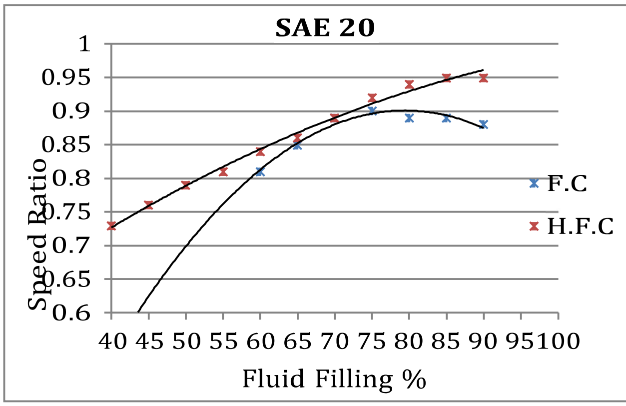


Fig.7: Effect of SAE 10 on speed ratios

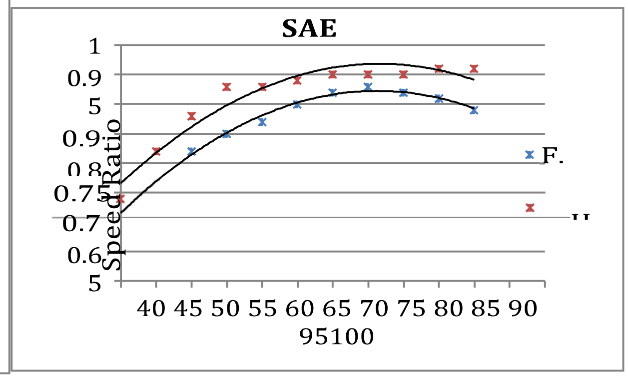


Fig.8: Effect of SAE 20 on speed ratios

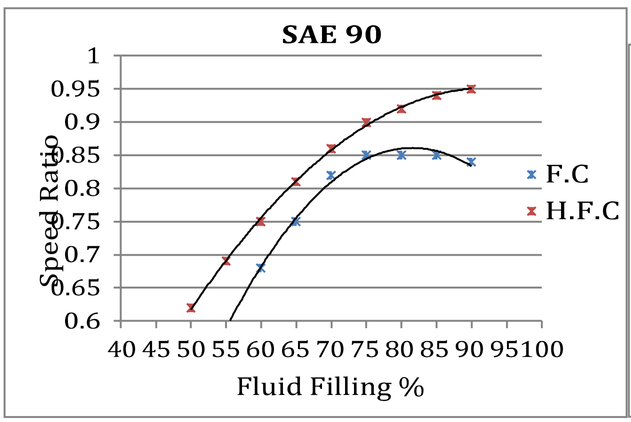


Fig. 9: Effect of SAE 40 on speed ratios

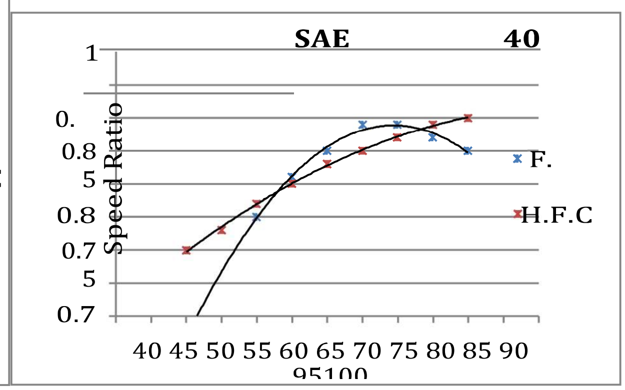


Fig. 10: Effect of SAE 90 on speed ratios

or all fluids (SAE 10, SAE 20, SAE 40, and SAE 90), it has been found that while filling capacity rises, speed ratios also increase until a certain point, at which point they both slightly decrease for fluid couplings with one input and two inputs. The findings indicate that fluids with lower viscosity, such as SAE 10 and SAE 20, yield a more favorable speed ratio, whereas fluids with higher viscosity, such as SAE 40 and SAE 90, result in a less desirable speed ratio. The Single Input Fluid Couple exhibits maximum speed ratios of 0.93 (as shown in Figure 7) and 0.90 (as shown in Figure 8) for SAE 10 and SAE 20, respectively. Similarly, for SAE 40 and SAE 90, the highest speed ratios are 0.89 (as depicted in Figure 9) and 0.85 (as illustrated in Figure 10), respectively. Figures 7 and 8 show the maximum speed ratios for SAE 10 and SAE 20 with Two Inputs Fluid Coupling, whereas Figures 9 and 10 show the maximum speed ratios for SAE 40 and SAE 90, both of which are 0.95. Fluids with low viscosity initiate the transfer of power when they are filled to low capacities.

Comparison of SAE 10 Power Output for Single and Two Input Fluid Couplings with Various Fluid Filling Capabilities:

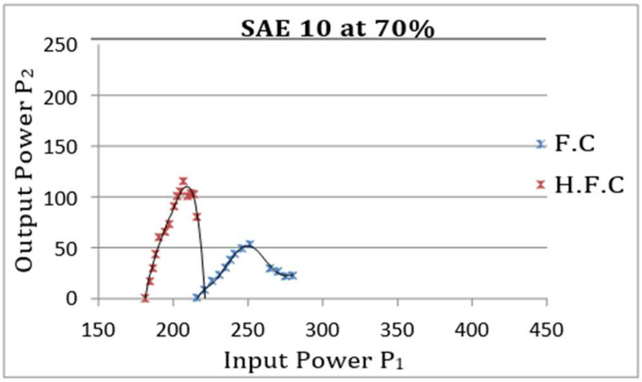


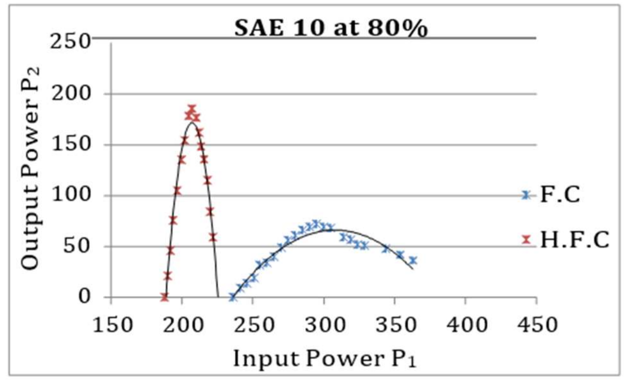


Fig. 11: Effect of SAE 10 on Output Power at Power at70% filling capacity

Fig. 12: Effect of SAE 10 on Output 80% filling capacity

Figs. 11, 12, and 13 show the output of SAE 10 at 70%, 80%, and 90% filling levels for both single-input interfaces and two-input interfaces. The data shown in these figures shows that the output of a two-input fluid coupling is greater than that of a single-input fluid coupling at varying filling capacities. As the storage capacity of the system grows, there is an initial increase in the output power up to a certain point, after which it subsequently decreases, as seen in the figures.

Comparison of SAE 20 Power Output at Various Fluid Filling Capabilities for Single and Dual Input Fluid Coupling

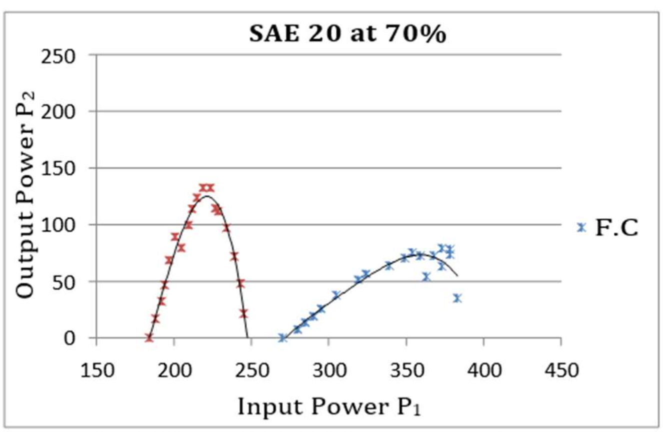


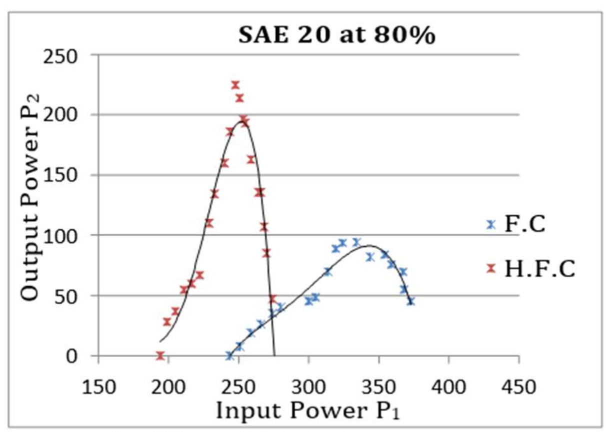


Fig. 14: Effect of SAE 20 on Output Power at Power at70% filling capacity

Fig. 15: Effect of SAE 20 on Output 80% filling capacity

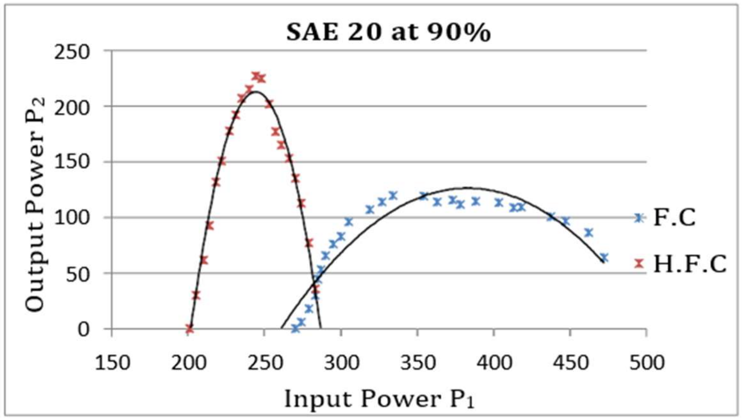


Fig. 16: Effect of SAE 20 on Output Power at90% filling capacity

Figures 14, 15, and 16 demonstrate the power output for SAE 20 at 70%, 80%, and 90% filling capacities for single and two input fluid couplings. The data shown in these figures demonstrates that the electrical output of the two-input fluid coupling surpasses that of the single-input fluid coupling across various filling capacities. As the filling capability is increased, the output power exhibits an initial increase up to a certain point, after which it subsequently decreases, as seen in the accompanying figures.

Comparison of SAE 40 Power Output between Single and Dual Input Fluid Couplings, with Increasing Fluid Filling Capacity

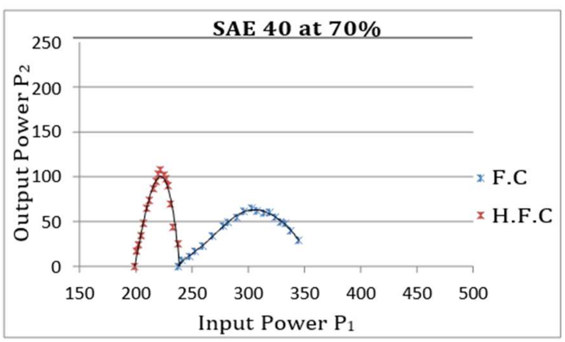


Fig. 17: Effect of SAE 40 on Output Power at Power at70% filling capacity

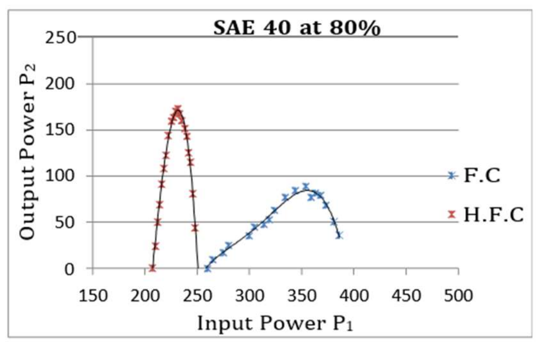


Fig. 18: Effect of SAE 40 on Output 80% filling capacity

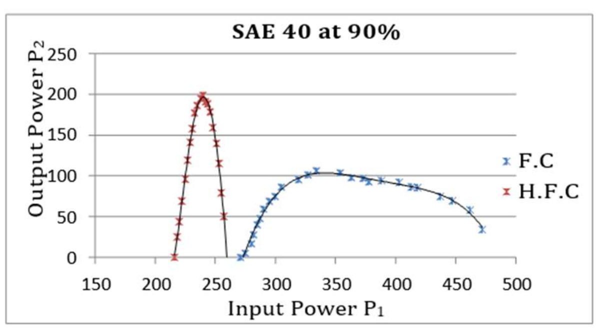


Fig. 19: Effect of SAE 40 on Output Power at 90% filling capacity

Figs. 17, 18, and 19 display the power output for SAE 40 at 70%, 80%, and 90% filling capacity for both single-input and two-input fluid couplings. These numbers show that the power output of the two-input fluid coupling is greater than that of the single-input fluid coupling throughout a wide range of fluid volumes. The statistics demonstrate that as the volume grows, the output power rises to a maximum before falling down.

Various fluid filling capacities and their effects on SAE 90 power output were compared for both single- and dual-input fluid couplings

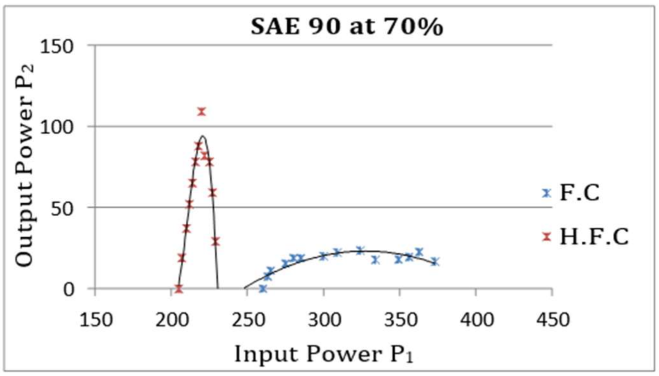


Fig. 20: Effect of SAE 90 on Output Power at Power at70% filling capacity

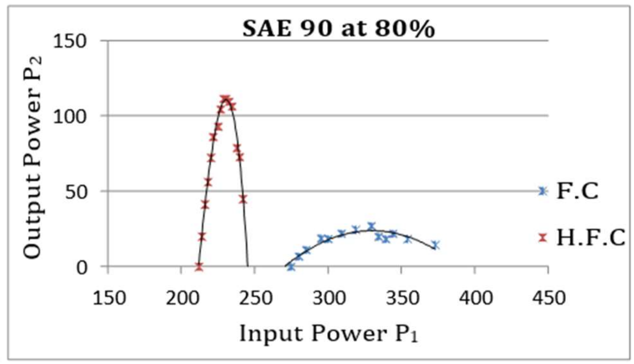


Fig. 21: Effect of SAE 90 on Output 80% filling capacity

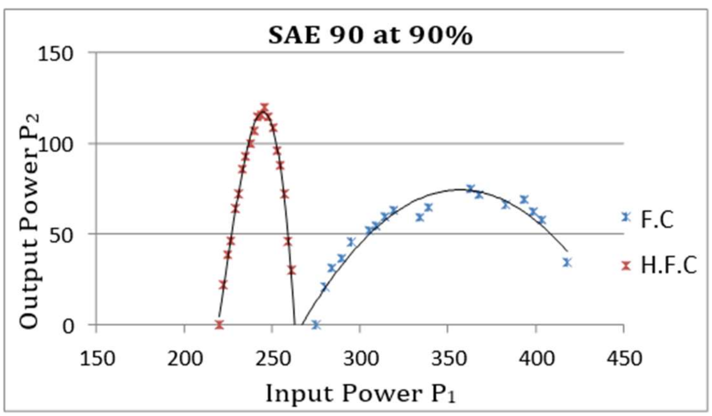


Fig. 22: Effect of SAE 90 on Output Power at 90% filling capacity

Tables 20, 21, and 22 display the power output for SAE 90 at filling capacities of 70%, 80%, and 90% for both single-input and two-input fluid couplings. These numbers show that the electrical output of the two-input fluid coupling is greater than that of the single-input fluid coupling throughout a wide range of fluid volumes. The statistics demonstrate that as the volume grows, the output power rises to a maximum before falling down.

**Table. 1:** Maximum Power Output for Single Input & Two Inputs Fluid Couplings

| **S.No.** | **Fluid** | **Filling Capacity (%)** | **Maximum Power Output (W)** | | |
|---|---|---|---|---|---|
| | | | **Single Input Fluid Coupling** | **Two Inputs Fluid Coupling** | **Fig. No.** |

| | | | | | |
|---|---|---|---|---|---|
| 1 | SAE 10 | 70 | 53 | 116 | 11 |
| 2 | | 80 | 72 | 190 | 12 |
| 3 | | 90 | 161 | 204 | 13 |
| 4 | SAE 20 | 70 | 75 | 132 | 14 |
| 5 | | 80 | 94 | 225 | 15 |
| 6 | | 90 | 116 | 227 | 16 |
| 7 | SAE 40 | 70 | 65 | 108 | 17 |
| 8 | | 80 | 89 | 173 | 18 |
| 9 | | 90 | 106 | 199 | 19 |
| 10 | SAE 90 | 70 | 24 | 109 | 20 |
| 11 | | 80 | 27 | 111 | 21 |
| 12 | | 90 | 75 | 120 | 22 |

Table 1 displays the highest power outputs for SAE 10, SAE 20, SAE 40, and SAE 90 Single Input and Two Input Fluid Couplings at 70%, 80%, and 90% filling capacities, respectively.

**Conclusions:**

Experimental studies on Single Input and Two Inputs Fluid Coupling with varied viscosity fluids and fluid filling capacities led to the aforementioned findings, which are summarized below.

1. The impact of the power source on the speed ratio is examined with the help of Figs. 5-8. It is found that the velocity ratio is higher for a two-input shaft fluid coupling than for a single-input shaft fluid coupling.
2. Based on the analysis of Figures 5-8, it can be noted that the rotational motion of the output shaft in the Two Inputs shaft Fluid Coupling initiates when the fluid linking is filled with a lesser capacity in comparison to the Single Input shaft Fluid Coupling.
3. Based on the analysis of Figures 9 to 20, it can be observed that the Two Inputs shaft Fluid Coupling exhibits a greater output power in comparison to the Single Input shaft Fluid Coupling.
4. The data indicates a positive correlation between the fluid filling capacity and the output power in both the Single Input and Two Inputs scenarios. A fluid coupling is a device used in mechanical engineering to transmit power between two rotating shafts. It operates by using a fluid medium
5. It has been noted that low viscosity fluids, such as SAE 10 and SAE 20, have a superior power transfer capability in both single input and two inputs scenarios. Fluid couplings are mechanical devices that transmit rotational power between two shafts using a fluid medium. They are commonly used in many industrial.

**References:**

1. Froude.W, On a New Dynamometer for measuring the power delivered to the screws of Large Ships. Proceedings of the Institution of Mechanical Engineers, Vol, 72, July 1877, pp. 237-252.

2. Dr.-Ing. Herrmann Fottinger, Discussion on "Recent Developments in Hydraulic Couplings", Proceedings of the Institution of Mechanical Engineers, Vol, 130, April 26, 1935, pp. 158-161.

3. Harold Sinclair, "Some Problems in the Transmission of Power by Fluid Couplings", Proceedings of the Institution of Mechanical Engineers, Vol. 139, April, 1938, pp. 83-157

4. J. Bilton, "Emptying Valves for Fluid Couplings", The Engineer, Vol. 217, No. 5644, 1964, pp. 576-577.

5. P. M. Heldt, "A Mathematical Consideration of the Fluid Coupling", Automotive Industries, Vol. 82, No. 8, 1940, pp. 360- 362, 384.

6. Patkl. G.S., Gill B.S., The Effect of Number of Blades on the performance of Hydrodynamic Couplings and Dynamometers. Mech. Engg. Bull. (India), Vol. 7, No. 3, Sept 1976, pp. 80-88.

7. Uchiyama, K. and Takaya, H. Internal flow in scoop tube of a fluid coupling. Bulletin of JSME, 1985, 51 (468), 2515-2522 (in Japanese). JMES1478R1: Analysis of Fluid Flow and Heat Transfer in Industrial Fluid Couplings Revised version for Journal of Mech. Engg. Sci. (Part C, Proc. IMechE)

8. Middelmann, V. Analysis des system verhaltens hydrodynamischer kupplungenbei variation der kreislaufgeometrie. PhD thesis, 1992, Ruhr-Universitat Bochum (in German).

9. Bai, L., Blomerius, H., Mitra, N.K. and Fiebig, M. Numerical simulation of unsteady incompressible 3D turbulent flow in fluid couplings with inclined blades. Proc. of the 1994 International Mechanical Engineering Congress and Exposition, ASME, Chicago, IL, USA, 6-11 November 1994, Dynamic Systems and Control Division (Publication) DSC, 55-2, Dynamic Systems and Control, 2 (2), 609-616.

10. Tanaji Balawant Shinde, Aditya Arvind Yadav, Anamika Mahadev Pol , Apeksha Baburao Kamble ”Design of fluid coupling for efficient transmission for mopeds” International Research Journal of Engineering and Technology (IRJET), Vol. 05, Issue 02, Feb 2018, pp. 727-730.

11. Zixiang SUN, John Chew, Neil Fomison and David Edwards “Analysis of Fluid Flow and Heat Transfer in Industrial Fluid Couplings” Revised version for Journal of Mech. Engg. Sci. –JMES 1478R1 (Part C, Proc. Inst. Mech. Engg.)

12. Er. Nitesh Jain, Dr. Aceem Tiwari, Comparative Study of Fluid Coupling for Oil and water as working fluid, International Journal of Engineering Research and Development, e-ISSN: 2278- 067X, p-ISSN: 2278-800X, Volume 9, Issue 6 (December 2013), PP. 56-61

13. Mr. Hirendra B. Patel, Dr.Pravin P.Rathod, Prof. Arvind .Sorathiya, Design and performance analysis of hydro-kinetic fluid coupling, / International Journal of Engineering Research and Applications (IJERA) ISSN: 2248-9622,Vol. 2, Issue 4, July-August 2012, pp.227-232

14. F. J. Wallace, A. Whitfield, R. Sivalingam. “A theoretical model for the performance prediction of fully filled fluid coupling” International journal of mechanical Science, Volume 20, Issue 6, 1978, Pages 335-347.

15. Ishihara. T, Emori. R.I. Torque Converter as a Vibration Damper and its Transient Characteristics. Trans SAE. No. 660368.
16. Uchiyama, K., Takagi, T. and Okazaki, T. Relationship between fluctuation of output shaft rotation speed and internal flow in fluid coupling of variable filling type. Bulletin of JSME, 1980, 46 (405), 893-901 (in Japanese).
17. Mohd. Mohinoddin , Naveed Wasay, S. Nawazish Mehdi, Shaik Shafee and Azam Ali, Design of fluid coupling for hybrid transmission systems, Global Journal of Mechanical Engineering and Computational Science– ISSN 2249-3468 GJMECS Vol.1 (3), 2011: pp.73-77
18. Syed Danish Mehdi, Dr. Mohd Mohinoddin, Dr.Syed Nawazish Mehdi, ―Investigations on the Fluid Coupling of Gearless Two Wheeler, International Journal of Scientific Engineering and Applied Science (IJSEAS) - Volume-1, Issue-7,October 2015 ISSN: 2395-3470, PP: 220-234
19. Hayder Kareem Sakran, Numerical Analysis of the Effect of the Numbers of Blades on the Centrifugal Pump Performance at Constant Parameters, International Journal of Mechanical Engineering and Technology , 6(8), 2015, pp.105-117.
20. V. Ramkumar, M.Prabhu, Study of the existing design of impeller of 4" submersible pump and improving its efficiency using CFD a through theoretical analysis, international journal of mechanical engineering and technology (IJMET) Volume 6, Issue 5, May (2015), pp. 51-55
21. Ji Pei, Fan Meng, Yanjun Li, Shouqi Yuan and Jia Chen, Fluid–structure coupling analysis of deformation and stress in impeller of an axial-flow pump with two-way passage, Advances in Mechanical Engineering, Vol.8(4) I-II, 2016, pp.1-11, DOI:10.1177/1687874016646266, aime.sagepub.com
22. Narayan Rao. N. N. The Basic Theory of Hydraulic Dynamometers & Retarders. Trans. SAE. Vol. 77, No. 680178.
23. Knudsen. D.D., Countess. R. B. Hydrodynamic Considerations in Water Dynamometer Design. Trans. SAE. Vol. 80,No. 710217.
24. Mitsuhashi. K., Takata N., Urushihara.A. Endo.Y., Kabayano.N. Vibration of Hydraulic Dynamometer and Resonant Response Factor.
25. T. F. Rolewicz, "Design of Hydrostatic Dynamometers for the Testing of Drive train Components," M.S. Thesis, University of Wisconsin, Madison, WI, 1987.
26. J. C. Longstreth, F. A. Sanders, S. P. Seaney, J. J. Moskwa and F. J. Fronczak, "Design and Construction of a High-Bandwidth Hydrostatic Dynamometer," SAE Technical Paper 930259, 1993.
27. M. A. Holland, K. Harmeyer and J. H. Lumkes, "Design of a High-Bandwidth, Low-Cost Hydrostatic Absorption Dynamometer with Electronic Load Control," SAE Technical Paper 2009-01-2846, 2009.
28. M. Maqableh, Mathematical Modeling of Partially Filled Fluid Coupling Behavior, World Academy of Science, Engineering and Technology, International Journal of Mechanical, Aerospace, Industrial, Mechatronic and Manufacturing Engineering Vol:5, No:12, 2011, pp. 2626-2631.

29. V. Narasimha Reddy, Dr. P. Ram Reddy, Dr. Syed Nawazish Mehdi, Optimization of Fluid Coupling performance for Hybrid Power Transmission system, IOSR Journal of Mechanical and Civil Engineering (IOSR-JMCE) e-ISSN: 2278-1684,P-ISSN:2320- 334X, Volume 14, Issue 4, Ver. III (Jul.- Aug. 2017), pp 39-44.